Received: 30 December 2022 | Revised: 23 January 2023 | Accepted: 25 January 2023

DOI: 10.1002/ar.25174

SPECIAL ISSUE ARTICLE

The Anatomical Record WILEY

The ear region of the Philippine flying lemur *Cynocephalus volans* (Placentalia, Dermoptera)

John R. Wible

Section of Mammals, Carnegie Museum of Natural History, Pittsburgh, Pennsylvania, USA

Correspondence
John R. Wible, Section of Mammals, Carnegie Museum of Natural History, 5800 Baum Boulevard, Pittsburgh, PA 15206, USA.
Email: wiblej@carnegiemnh.org

Funding information
National Science Foundation, Grant/Award Number: DEB 1654949

Abstract

The placental order Dermoptera, which includes two extant species, the Philippine and Sunda flying lemurs, *Cynocephalus volans* and *Galeopterus variegatus*, respectively, is generally held to be the sister group of Primates. Yet, little has been reported on their cranial anatomy. Here, the anatomy of the ear region is described and illustrated for a juvenile and adult *C. volans* based on CT scans. The inclusion of a juvenile is essential as nearly all cranial sutures are fused in the adult. Soft tissues are reconstructed based on sectioned histological pre- and postnatal specimens previously reported by the author. Numerous unusual features are identified, including: a small parasphenoid beneath the basisphenoid, a tensor tympani fossa on the epitympanic wing of the squamosal, a cavum supracochleare for the geniculate ganglion of the facial nerve that is not enclosed in the petrosal bone, a secondary facial foramen between the petrosal and squamosal, a secondary posttemporal foramen leading to the primary one, a subarcuate fossa that is floored in part by a large contribution from the squamosal, a body of the incus larger than the head of the malleus, and a crus longum of the incus that lacks an osseous connection to the lenticular process. Documentation of the anatomy of the Philippine flying lemur ear region is an essential first step in morphological phylogenetic analyses where features of the basicranium are widely sampled.

KEYWORDS

facial nerve, incus, lenticular process, malleus, petrosal, posttemporal foramen

1 | INTRODUCTION

The order Dermoptera includes two extant species (Stafford, 2005), the Philippine flying lemur *Cynocephalus volans* (Linnaeus, 1758), and the Sunda flying lemur *Galeopterus variegatus* (Audebert, 1799). Molecular phylogenetic analyses have identified flying lemurs (or colugos) as the sister group of Primates (e.g., Álvarez-Carretero et al., 2022; Murphy et al., 2021), whereas the one recent combined analysis of molecules and morphology (O'Leary et al., 2013) has Primates outside of Sundatheria, a Dermoptera and Scandentia (treeshrews) clade.

Despite their close evolutionary relationships to Primates, dermopterans have not received much recent attention from comparative morphologists. Regarding cranial osteology, for example, the major references are more than 100 years old (Leche, 1886; Schuffeldt, 1911). Regarding the ear region, the subject of this report, the most comprehensive study is that of Hunt and Korth (1980), who considered both morphology and function. These authors provided a detailed accounting of the prior literature, including the ontogenetic studies by Parker (1885) and Klaauw (1922), considered the major auditory features of the middle ear, and made a case for lower

frequency hearing adaptations. Since their comprehensive study, there have only been a handful of contributions relevant to the topic. MacPhee et al. (1989) provided labeled photographs of the basicranium of *C. volans*, with and without the bulla in place, and discussed ear region features in the context of describing an early Eocene plagiomenid fossil. Wible (1993) studied the nerves and vessels of the ear region of four serially sectioned pre- and postnatal specimens; two were from the Philippines and, therefore, are *Cynocephalus*, but locality information for the other two was lacking. Using the same sectioned specimens plus an additional postnatal one, Wible and Martin (1993) reported on the development of the tympanic floor and roof. Diogo (2009) detailed the cranial musculature based on two adult *C. volans*. Ekdale (2013) included *C. volans* in his broad comparative treatment of the inner ear in placental mammals. Lastly, Silcox et al. (2020: figure 20.2) published a CT slice through the mastoid of *C. volans*, illustrating the extreme pneumatization of this area of the cranium.

Despite these contributions, much of the dermopteran ear region remains incompletely or poorly described. Complicating investigation is the fusion between basicranial bones in adult flying lemurs, making it impossible to fully delimit individual elements. Additionally, the complete enclosure of the middle ear by the auditory bulla obscures numerous features sampled in morphological phylogenetic analyses. To address these complications, I studied CT scans of a juvenile and adult *C. volans* along with the histological specimens reported in Wible (1993; see also Wible & Martin, 1993). The ontogenetic trajectory allowed for the delimitation of most basicranial bones, and the segmentation function of the computer software allowed for the illustration of these individual elements.

2 | MATERIALS AND METHODS

2.1 | Specimens

CT scans were studied of the following specimens:

1. *Cynocephalus volans*, AMNH 187861, juvenile female, collected August 1, 1961 in Mt. Lobi, Leyte, Philippines. The skull was scanned on the Nikon Metrology XT H 225 ST, Duke Shared Materials Instrumentation Facility, Duke University. Doug Boyer provided access to these data originally appearing in NSF BCS 1552848. The files, MorphoSource Media 000025387, were downloaded from www.MorphoSource.org, Duke University. The CT image series included 1,664 tiff images. X, Y, and Z spacing is 0.037368 mm. Hunt and Korth (1980) identified this specimen as an adult female, but it is clearly a juvenile with the first and second lower incisors deciduous with replacement teeth below them, and although three upper and lower molars are present, they are unerupted and without roots.
2. *Cynocephalus volans*, FMNH 56442, adult female, collected December 10, 1946 in South Cotabato Province, Mindanao, Philippines. The cranium was scanned on the Nikon Metrology XT H 225 ST, Duke Shared Materials Instrumentation Facility, Duke University. Doug Boyer provided access to these data, the collection of which was funded by NSF BCS 1317525 (to DM Boyer and ER Seiffert), 1552848 (to DM Boyer), and Duke University Trinity College of Arts and Sciences. The files, MorphoSource Media 000034323, were downloaded from www.MorphoSource.org, Duke University. The CT image series included 2,789 tiff images. X, Y, and Z spacing is 0.026666 mm.

Histological slides were studied of the following specimens (see also Wible, 1993; Wible & Martin, 1993):

1. *Cynocephalus volans*, DUCEC 804, prenatal. Head was embedded in paraffin and sectioned in a frontal plane at 15 μm. Stain: Mallory's trichrome. Crown-rump length (CRL): 88 mm. Head length (HL): 28 mm. [Although listed as *Cynocephalus variegatus*, this specimen is said to be from the Philippines and, therefore, should be *Cynocephalus volans*.]
2. *Cynocephalus* sp., DUCEC 8310, prenatal. As above, but CRL: 107 mm. [No locality data.]
3. *Cynocephalus volans*, DUCEC 806, neonate or postnatal. As above, but right half of head sectioned in a sagittal plane at 20 μm and left half in a frontal plane at 15 and 20 μm. Stain: Azan. CRL: 136 mm. HL: 44 mm. [Although listed as *Cynocephalus variegatus*, this is specimen is said to be from the Philippines and, therefore, should be *Cynocephalus volans*.]
4. *Cynocephalus* sp., DUCEC 839, neonate or postnatal. As above, but whole head sectioned in a frontal plane at 20 and 40 μm. Stain: Azan. CRL: 150 mm. HL: 49 mm. [No locality data.]

I reiterate the concerns already raised by Wible (1993) and Wible and Martin (1993) about the taxonomic identification of the two histological specimens reported as *Cynocephalus* sp. I have not found any features in these two specimens that can help in distinguishing between *Cynocephalus* and *Galeopterus*. In order to highlight this uncertainty for the reader, I refer to these two specimens as "*Cynocephalus*" in the text.

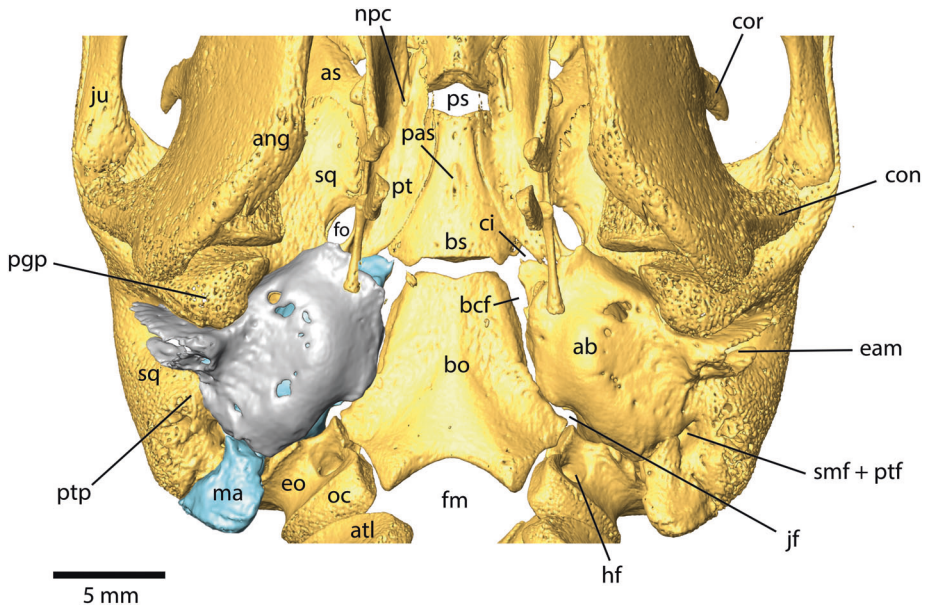

FIGURE 1 *Cynocephalus volans*, AMNH 187861, isosurface derived from the CT scans of the basicranium, dentary, and hyoid elements in ventral view. Braincase roof is removed to help visualize foramina and spaces. Right auditory bulla and osseous external acoustic meatus are in gray and the right petrosal is in light blue. Abbreviations: ab, auditory bulla; ang, angular process; as, alisphenoid; atl, atlas; bcf, basicapsular fissure; bo, basioccipital; bs, basisphenoid; ci, carotid incisure; con, condylar process; cor, coronoid process; eam, external acoustic meatus; eo, exoccipital; fm, foramen magnum; fo, foramen ovale; hf, hypoglossal foramen; jf, jugular foramen; ju, jugal; ma, mastoid; npc, for nerve of pterygoid canal; oc, occipital condyle; pas, parasphenoid; pgp, postglenoid process; ps, presphenoid; pt, pterygoid; ptp, posttympanic process; smf + ptf, opening to stylomastoid and posttemporal foramina; sq, squamosal.

Crania were studied of the following specimens:

1. *Galeopterus variegatus*, CM 87908, adult female, collected August 6, 1983 in Surat Thani Province, Thailand.
2. *Galeopterus variegatus*, CM 87909, adult male, collected August 9, 1983 in Surat Thani Province, Thailand.

2.2 | Terminology

Anatomical terminology follows that used in prior publications by the author and collaborators (e.g., Wible, 1990, 2003; Wible & Shelley, 2020). Usage of English equivalents of the Nomina Anatomica Veterinaria (2017) is preferred when appropriate. Terms for the middle-ear ossicles follow Henson (1961).

2.3 | Institutional abbreviations

- AMNH, American Museum of Natural History, New York, NY, USA.
- CM, Carnegie Museum of Natural History, Pittsburgh, PA, USA.
- DUCEC, Duke University Comparative Embryological Collection, Durham, NC, USA.
- FMNH, Field Museum of Natural History, Chicago, IL, USA.

3 | DESCRIPTIONS

3.1 | *Cynocephalus volans*, AMNH 187861

In adult colugos, most bones of the basicranium lack sutures delimiting them from their neighbors (Hunt & Korth, 1980). In contrast, AMNH 187861, a juvenile female, has sutures between bones (Figure 1) with the following exceptions: the auditory bulla, which is known to be a composite of three elements based on prenatal specimens (Hunt & Korth, 1980; Klaauw, 1922; Wible & Martin, 1993), is a single entity, and the petrosal, squamosal, and ectotympanic component of the bulla are partially fused posterior to the external acoustic meatus.

The midline bones of the basicranium from anterior to posterior are the presphenoid, basisphenoid, and basioccipital; broad gaps between these are the synchondroses that were filled with cartilage in life (names of synchondroses indicated in Figure 2). The basisphenoid has a low, short midline ridge on its ventral surface

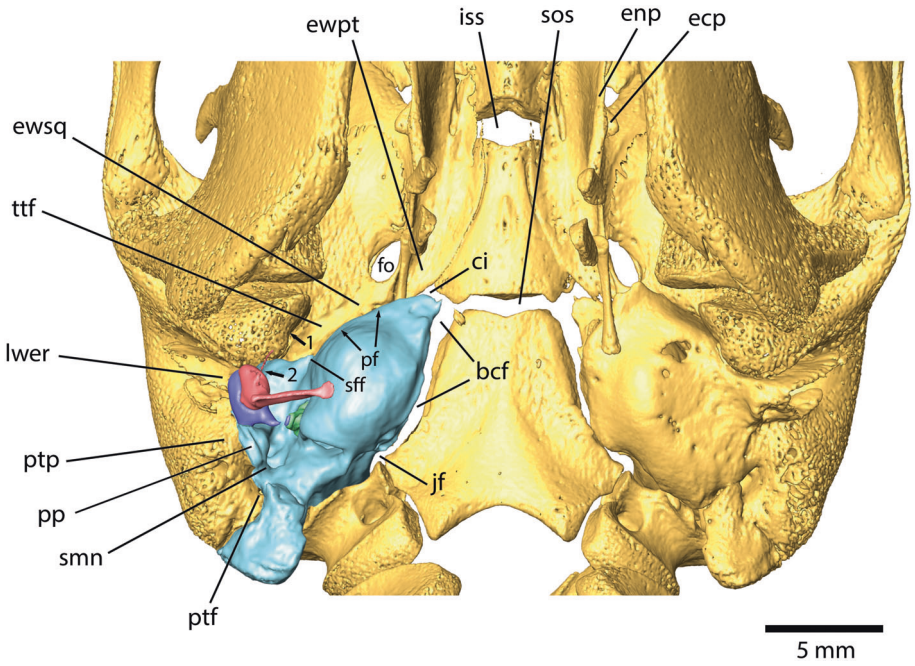

FIGURE 2 *Cynocephalus volans*, AMNH 187861, isosurface derived from the CT scans of the basicranium, dentary, and hyoid elements in ventral view. Braincase roof is removed to help visualize foramina and spaces. Right auditory bulla and osseous external acoustic meatus are removed; the right petrosal is in light blue; the right malleus, incus, and stapes are red, dark blue, and green, respectively. Arrow 1 shows opening to epitympanic sinus of squamosal; arrow 2 is to epitympanic recess. Abbreviations: bcf, basicapsular fissure; ci, carotid incisure; ecp, ectopterygoid process; enp, entopterygoid process; ewpt, epitympanic wing of pterygoid; ewsq, epitympanic wing of squamosal; fo, foramen ovale; iss, intersphenoid synchrondrosis; jf, jugular foramen; lwer, lateral wall of epitympanic recess; pf, piriform fenestra; pp, paroccipital process; ptf, posttemporal foramen; ptp, posttympanic process; sff, secondary facial foramen; smn, stylomastoid notch; sos, spheno-occipital synchrondrosis; ttf, tensor tympani fossa.

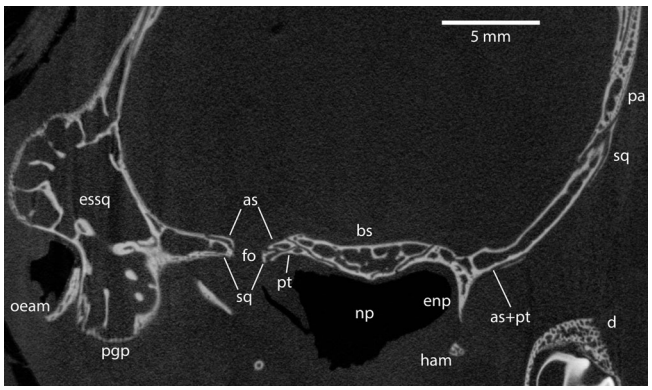

FIGURE 3 *Cynocephalus volans*, AMNH 187861, CT slice 1314 in oblique transverse plane. Left side of image is through foramen ovale, and right side is more anteriorly placed. Abbreviations: as, alisphenoid; bs, basisphenoid; d, dentary; enp, entopterygoid process; essq, epitympanic sinus of squamosal; fo, foramen ovale; ham, pterygoid hamulus; np, nasopharynx; oeam, osseous external acoustic meatus; pa, parietal; pgp, postglenoid process; pt, pterygoid; sq, squamosal.

(Figure 1). The prenatal specimens (*C. volans*, DUCEC 804 and "*Cynocephalus*," DUCEC 8310) have a tiny, independent dermal ossification here, the parasphenoid (see Parker, 1885; Wible et al., 2018), that is presumably fused to the basisphenoid in the older specimens (*C. volans*, DUCEC 806 and "*Cynocephalus*," DUCEC 839), including AMNH 187861.

Lateral to the basisphenoid are the pterygoid, alisphenoid, and squamosal (Figure 1). The pterygoid underlies the basisphenoid and is fused to the alisphenoid in some sections and separate in others (Figure 3). Wible and Martin (1993) reported the pterygoid and alisphenoid as fully separate in the prenatal specimens (*C. volans*, DUCEC 804, and "*Cynocephalus*," DUCEC 8310). In AMNH 187861, the pterygoid/alisphenoid is separated from the basisphenoid by sutures, endo- and extracranially (Figures 1, 3 and 4a); this is also the case in the pre- and postnatal specimens studied here and was reported by Parker (1885) in a 5.5 in. embryo of *Galeopithecus volans* (=*C. volans*). A pair of prominent entopterygoid crests extends ventrally from the basicranium to form the lateral walls of the basipharyngeal canal (for the nasopharynx) (Figures 2 and 3). The part of the entopterygoid crest visible in Figure 2 is formed primarily by the pterygoid, but is partially overlapped laterally by the alisphenoid (based on *C. volans*, DUCEC 804, and "*Cynocephalus*," DUCEC 8310). There are two processes on the entopterygoid crest: a

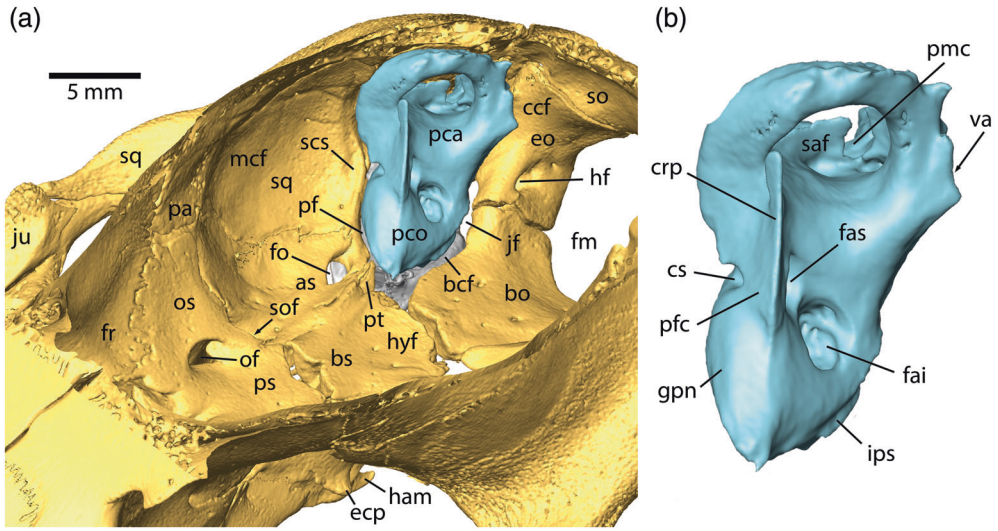

FIGURE 4 *Cynocephalus volans*, AMNH 187861, isosurfaces derived from the CT scans of endocranial surfaces in oblique anterolateral views. (a) Floor and right lateral wall with right petrosal in blue. (b) Right petrosal. Abbreviations: as, alisphenoid; bcf, basicapsular fissure; bo, basioccipital; bs, basisphenoid; ccf, caudal cranial fossa; crp, crista petrosa; cs, cavum supracochleare; ecp, ectopterygoid process; eo, exoccipital; fai, foramen acusticum inferius; fas, foramen acusticum superius; fm, foramen magnum; fo, foramen ovale; fr, frontal; gpn, for greater petrosal nerve; ham, pterygoid hamulus; hf, hypoglossal foramen; hyf, hypophyseal fossa; ips, for inferior petrosal sinus; jf, jugular foramen; ju, jugal; mcf, middle cranial fossa; of, optic foramen; os, orbitosphenoid; pa, parietal; pca, pars canalicularis; pco, pars cochlearis; pf, piriform fenestra; pfc, prefacial commissure; pmc, petromastoid canal; ps, presphenoid; pt, pterygoid; saf, subarcuate fossa; scs, sinus communicans sulcus; so, supraoccipital; sof, sphenorbital fissure; sq, squamosal; va, vestibular aqueduct.

short ectopterygoid process on the lateral surface on the alisphenoid (Figure 2) and a hook-shaped hamular process of the pterygoid at the posteroventral aspect (hidden in Figures 1 and 2 by hyoid elements but visible in Figure 4a). Lateral to the entopterygoid crest and underlying the alisphenoid is the medially expanded squamosal. A prominent structure in this surface is the foramen ovale for the mandibular nerve (Figure 2). The bones forming the foramen differ on the endo- and extracranial surfaces (Figure 3); the squamosal forms the bulk of the external aperture, with only a small contribution along the medial border from the alisphenoid, whereas the alisphenoid forms much of the internal aperture with a larger contribution to the posterior border from the squamosal (Figure 4a). Lateral to the foramen ovale is the mediolaterally broad glenoid fossa for the mandibular condyle (Figure 1), which is bordered posteriorly by the prominent postglenoid process (Figure 2). A postglenoid foramen is lacking.

Posterior to the auditory bulla from medial to lateral are the basioccipital, exoccipital, mastoid portion of the petrosal, and squamosal (Figure 1); the first three are well separated by sutures with the petrosal and squamosal partially fused. The occipital condyle is primarily on the exoccipital but with a small portion on the adjacent basioccipital. Anterior to the condyle is the single hypoglossal foramen within the exoccipital, transmitting the hypoglossal nerve and posterior meningeal artery and vein (Wible, 1993). Anterior to the hypoglossal foramen is the jugular foramen between the bulla, basioccipital, and exoccipital for the internal jugular vein and cranial nerves IX, X, and XI (Wible, 1993). There is a gap in the posterolateral aspect of the auditory bulla between the bulla, squamosal, and mastoid portion of the petrosal. This gap opens anteriorly into the middle ear and dorsally into a foramen between the petrosal and squamosal, and represents the combined stylomastoid and posttemporal foramina (Figures 1 and 2; see below).

The right auditory bulla, the floor of the middle ear, is removed in Figure 2 to expose the contents and roof of the middle ear, which includes the petrosal and the three middle-ear ossicles. Most of the anterior and medial surfaces of the petrosal do not directly contact neighboring basicranial bones; the remaining surfaces of the petrosal are wedged between the exoccipital posteromedially and the squamosal laterally. The medial border of the petrosal is separated from the basioccipital by a visible gap. The bulk of this gap is the basicapsular fissure, but it is continuous posteriorly with the jugular foramen and anteriorly with the carotid incisure. The carotid incisure between the petrosal, pterygoid, and basisphenoid transmits the internal carotid neurovascular bundle. In most mammals, the internal carotid artery (and accompanying sympathetic nerves) extends across the basicranium from the neck and enters the braincase to supply the cerebral circulation (Wible, 1986). In the four histological specimens studied by Wible (1993), the internal carotid artery

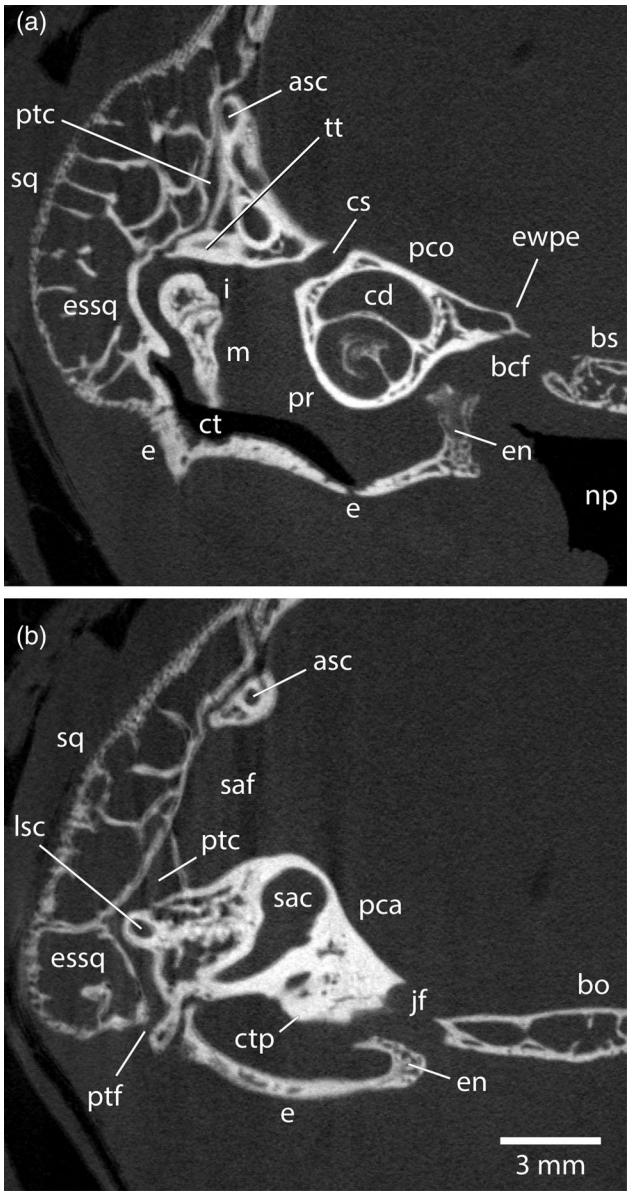

FIGURE 5 *Cynocephalus volans*, AMNH 187861, CT slices in oblique transverse plane. (a) Left side of image of slice 1380 through pars cochlearis; space over malleus and incus is the epitympanic recess. (b) Left side of image of slice 1484 through pars canalicularis; subarcuate fossa is floored by squamosal. Scale is for both slices. Abbreviations: asc, anterior semicircular canal; bcf, basicapsular fissure; bs, basisphenoid; bo, basioccipital; cd, cochlear duct; cs, cavum supracochleare; ct, cavum tympani; ctp, caudal tympanic process; e, ectotympanic; en, entotympanic; essq, epitympanic sinus of squamosal; ewpe, epitympanic wing of petrosal; i, incus; jf, jugular foramen; lsc, lateral semicircular canal; m, malleus; np, nasopharynx; pca, pars canaclicularis; pco, pars cochlearis; pr, promontorium; ptc, posttemporal canal; ptf, posttemporal foramen; sac, saccule; saf, subarcuate fossa; sq, squamosal; tt, tegmen tympani.

is incomplete and represented by only a tiny, short stump that leaves the cerebral circulation and enters the anterior middle ear. There is a tiny gap along the anterior aspect of the petrosal that is hidden in ventral view by horizontal shelves, epitympanic wings, on the rear of the pterygoid and squamosal. These wings do not contact the petrosal but partially underlie it, delimiting a narrow piriform fenestra, which is continuous medially with the carotid incisure (and therefore, the basicapsular fissure and jugular foramen). The sliver of piriform fenestra is visible in the oblique endocranial view in Figure 4a. The epitympanic wing of the squamosal has an elongate depression that based on *C. volans*, DUCEC 806, is the fossa for the tensor tympani muscle (Figure 2).

There are two other hidden spaces continuous with the middle ear indicated by arrows in Figure 2. Arrow 1 points to an enormous hidden aperture (foramen pneumaticum of Klaauw, 1931; epitympanic foramen of Hunt & Korth, 1980) that opens into an extensive epitympanic sinus (Figure 3) filling the interior of the squamosal bone, from the posterior zygomatic root to the occiput; this aperture is nearly completely in the squamosal with only a tiny petrosal contribution from the anterior tip of the tegmen tympani. Arrow 2 points to the epitympanic recess, the space over the mallear-incudal articulation, which is formed by the petrosal and squamosal bones (Figure 5a), and is largely hidden in the illustrated view.

The petrosal and middle-ear ossicles are isolated from the basicranium in ventral view in Figure 6. I divide the petrosal into two parts, the pars cochlearis housing the cochlea and saccule and the pars canalicularis housing the semicircular canals and utricle; this is equivalent to the petrous and mastoid portions of others (e.g., MacIntyre, 1972). The main feature on the pars cochlearis is the bulbous promontorium (Figure 6a), reflecting the encased cochlea (Figures 5a and 6b). Ekdale (2013) reported the cochlea of *C. volans* to be coiled 954°; the cochlea of AMNH 187861 is coiled 946°, using Ekdale's (2013) method. The ventral promontorial surface has two main prominences angled anteromedially (Figure 6a), the posterior one being the basal cochlear coil (Figure 6b). The ventral surface also has two narrow grooves that diverge from a common groove posteriorly and reunite anteriorly (Figure 6a), similar to the course of the internal carotid nerves illustrated for *C. volans*, DUCEC 806, by Wible (1993: figure 6a; see also Hunt & Korth, 1980: figure 16). Reaching anteromedially from the promontorium is a triangular shelf, the epitympanic wing of the petrosal. Based on *C. volans*, DUCEC 806, the internal carotid nerves cross the lateral aspect of the epitympanic wing, whereas the medial surface contacts the cartilage of the auditory tube.

The rear of the promontorium is breached by two openings, the round and oval windows (Figure 6a). The round window or fenestra cochleae is a nearly vertical opening in the posterior surface; it is oval with a length

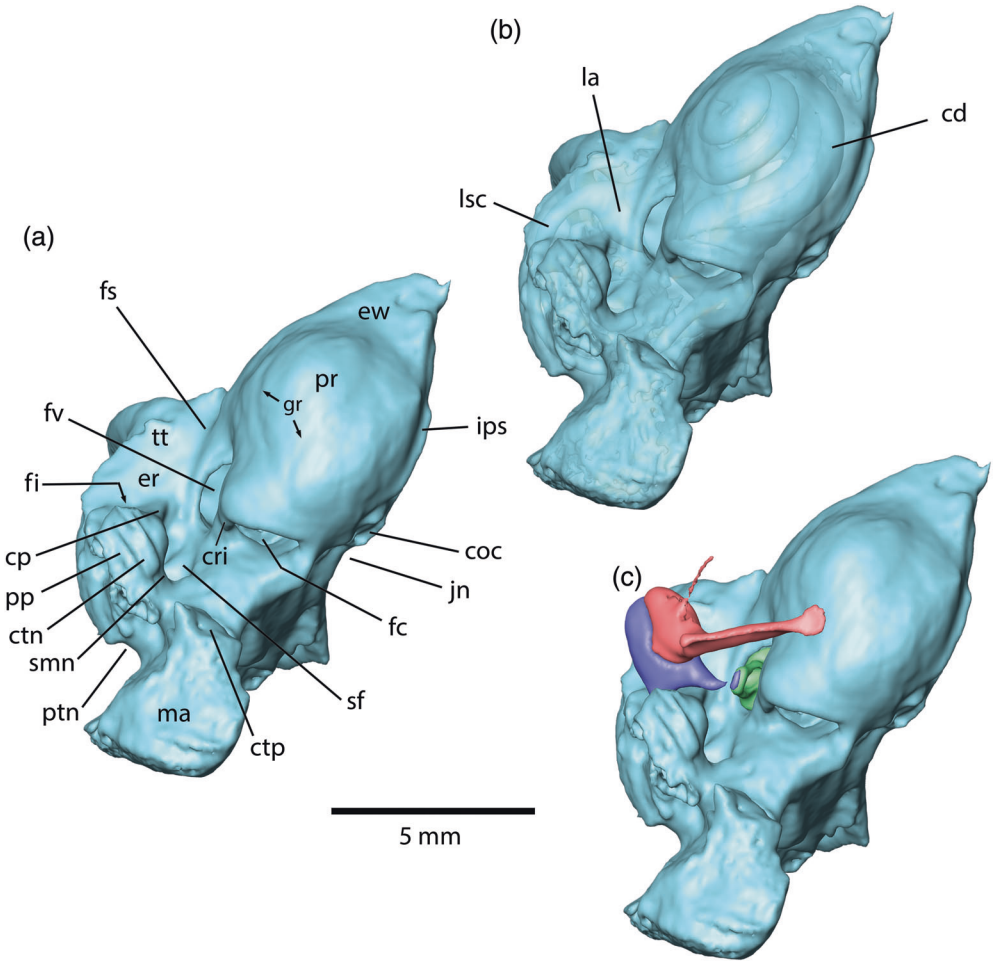

FIGURE 6 *Cynocephalus volans*, AMNH 187861, isosurfaces derived from the CT scans of right petrosal in ventral view. (a) Shaded; (b) transparent; (c) with malleus, incus, and stapes in red, dark blue, and green, respectively. Abbreviations: cd, cochlear duct; coc, cochlear canaliculus; cp, crista parotica; cri, crista interfenestralis; ctn, for chorda tympani nerve; ctp, caudal tympanic process; er, epitympanic recess; ew, epitympanic wing; fc, fenestra cochleae; fi, fossa incudis; fs, facial sulcus; fv, fenestra vestibuli; gr, grooves for internal carotid nerves; ips, for inferior petrosal sinus; jn, jugular notch; la, lateral ampulla; lsc, lateral semicircular canal; ma, mastoid; pp, paroccipital process; pr, promontorium; ptn, posttemporal notch; sf, stapedius fossa; smn, stylomastoid notch; tt, tegmen tympani.

to width ratio of 1.48. The dorsal surface at the round window is smooth; a cochlear fossula is absent. The oval window or fenestra vestibuli is slightly smaller and lies in the posterolateral surface. It is best seen in lateral view (Figure 7a). The oval window, which accommodates the footplate of the stapes, is obliquely oriented, closer to horizontal than vertical, with a stapedial ratio (Segall, 1970), length to width, of 1.60. It is recessed from the promontorial surface, producing a vestibular fossula, best developed on the dorsal aspect. The bone separating the two windows, the crista interfenestralis, is narrower than the longest dimensions of either window.

In ventral view (Figure 6a), the pars canalicularis is lateral and posterior to the promontorium. Centrally position on the pars canalicularis is a rounded prominence, the paroccipital process, which is covered by and fused to the posttympanic process of the squamosal laterally (Figure 2) and to the ectotympanic portion of the bulla ventrally (Figure 1). Medial to the paroccipital process is a large, oval depression (longer than wide), the fossa for the stapedius muscle, that is subdivided by a transverse crest; only the anterior half of this fossa is visible in the ventral view (Figure 6a). Extending and decreasing in height anteriorly from the paroccipital process is the crista parotica (Figures 6a and 7a), which typically is the site of attachment of the tympanohyal, the proximal segment of Reichert's cartilage (Moore, 1980); AMNH 187861 has no sign of a tympanohyal, also reported to be absent in the pre- and postnatal specimens studied by Wible and Martin (1993). Lateral to the crista parotica is the petrosal's contribution to the epitympanic recess, which is roofed by the diminutive tegmen tympani (Figures 5a, 6a and 7a). A small depression, the fossa incudis, that accommodates the crus breve of the incus sits posterior to the epitympanic recess on the anterior face of the paroccipital process (Figure 6a,b). Forming the dorsal base of the paroccipital process and tegmen tympani is the gyrus of the lateral semicircular canal (Figure 6c).

The rear of the pars canalicularis is dominated by the large, quadrangular mastoid portion of the petrosal. Based on *C. volans*, DUCEC 806, the ventral surface of the mastoid provides attachment for the posterior digastric and jugulohyoideus muscles (see also Diogo, 2009). The mastoid houses a large sinus that is continuous with the epitympanic sinus of the squamosal via several small

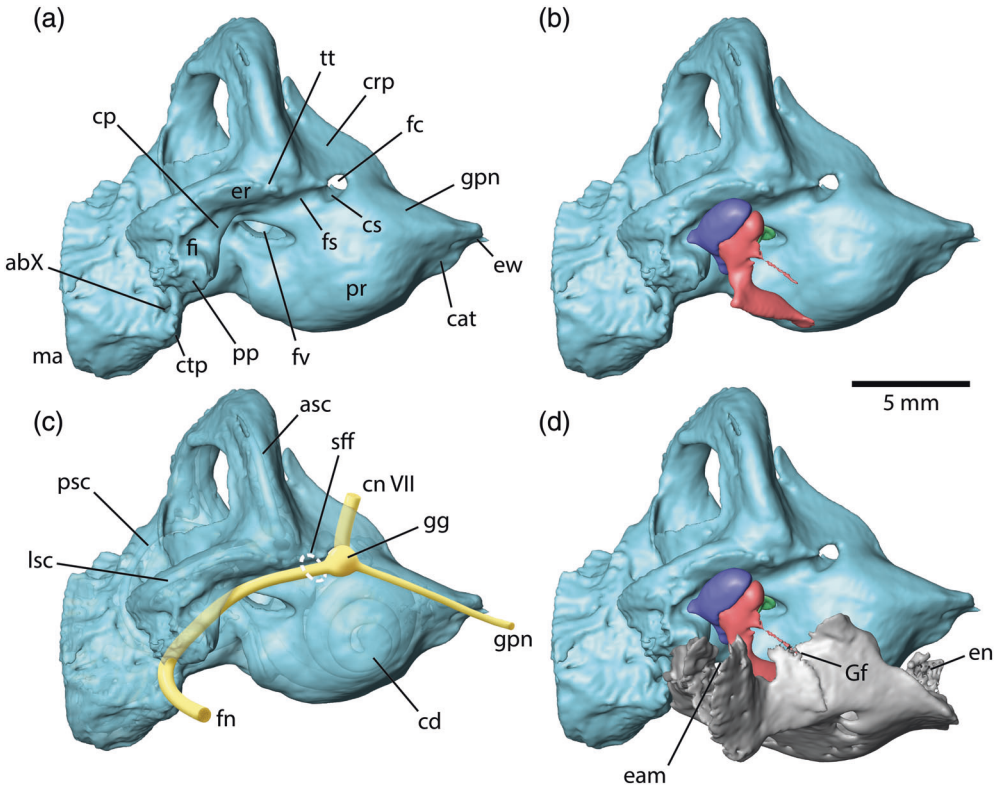

FIGURE 7 *Cynocephalus volans*, AMNH 187861, isosurfaces derived from the CT scans of right petrosal in lateral view. (a) Shaded; (b) with malleus, incus, and stapes in red, dark blue, and green, respectively; (c) transparent, with cranial nerve VII reconstructed based on *C. volans*, DUCEC 804, 806; (d) with auditory bulla and osseous external acoustic meatus added to (b). Abbreviations: abX, for auricular branch of vagus; asc, anterior semicircular canal; cat, for cartilage of auditory tube; cd, cochlear duct; cn VII, cranial nerve VII; cp, crista parotica; crp, crista petrosa; cs, cavum supracochleare; ctp, caudal tympanic process; eam, external acoustic meatus; en, entotympanic; er, epitympanic recess; ew, epitympanic wing; fc, facial canal; fi, fossa incudis; fn, facial nerve; fs, facial sulcus; fv, fenestra vestibuli; Gf, Glaserian fissure; gg, geniculate ganglion; gpn, greater petrosal nerve or sulcus; lsc, lateral semicircular canal; ma, mastoid; pp, paroccipital process; pr, promontorium; psc, posterior semicircular canal; sff, position of secondary facial foramen formed between petrosal and squamosal; tt, tegmen tympani.

openings on the lateral aspect of the mastoid (Figure 7). In lateral view (Figure 7a), the mastoid projects farther ventrally than the promontorium and is separated from the promontorium by a concavity. The anterior vertical wall of the mastoid, which forms the rear of the concavity, represents the caudal tympanic process of the petrosal (Figure 5b), marking the posterior limit of the middle ear. There is a small canal that runs mediolaterally through the caudal tympanic process base (Figure 7a), connecting the jugular and stylomastoid foramina. The nerve in this position in *C. volans*, DUCEC 806, is the auricular branch of the vagus (Wible, 1993: figure 6A), although this postnatal specimen does not have a separate canal for the nerve as occurs in AMNH 187861. In ventral view (Figure 6a), the caudal tympanic process is separated from the paroccipital process by a gap, which is closed to a foramen by the bulla (Figure 1). It is through this gap that the facial nerve exits the middle ear (see below) and the arteria and vena diploëtica magna enter the posttemporal foramen between the petrosal and squamosal. The paroccipital process and caudal tympanic process are the only points of contact that the bony auditory bulla has with the petrosal.

An important structure traversing the petrosal is cranial nerve VII and its primary branches (Figure 7c). This nerve's course begins on the petrosal's endocranial surface at the foramen acusticum superius within the shallow internal acoustic meatus (Figure 4b). It enters the facial canal, which runs anterolaterally through the base of the prefacial commissure, on top of which is the prominent crista petrosa (to which the tentorium cerebelli is attached). At the end of the facial canal is a depression in the petrosal that houses the geniculate ganglion of the facial nerve (Figures 4b and 7a,c). This depression represents the cavum supracochleare (Gaupp, 1905), which is unusual among therians in that it lies within the endocranium and not within the petrosal (Wible, 1990; Wible & Hopson, 1993). The geniculate ganglion has

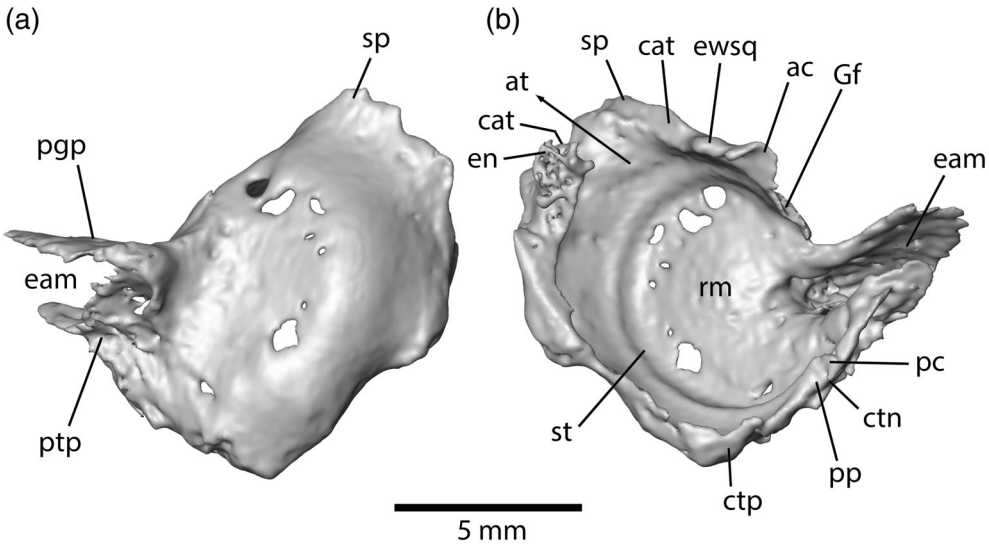

FIGURE 8 *Cynocephalus volans*, AMNH 187861, isosurfaces derived from the CT scans of right auditory bulla and osseous external acoustic meatus. (a) Ventral view; (b) dorsal view. Abbreviations: ac, anterior crus; at, for auditory tube; cat, for cartilage of auditory tube; ctn, for chorda tympani nerve; ctp, for caudal tympanic process; eam, external acoustic meatus; en, entotympanic; ewsq, for epitympanic wing of squamosal; Gf, Glaserian fissure; pc, posterior crus; pgp, for postglenoid process; pp, for paroccipital process; ptp, for posttympanic process; rm, recessus meatus; sp, for styliform process; st, sulcus tympanicus.

anterior and posterior branches. The smaller anterior branch is the greater petrosal nerve, which runs endocranially in a faint groove on the pars cochlearis (Figures 4b and 7a,c); at the carotid incisure, it joins a branch of the internal carotid nerve to form the nerve of the pterygoid canal (see Wible, 1993: figure 6A). The larger posterior branch of the ganglion is the main continuation of the facial nerve. It leaves the cavum supracochleare and enters the middle ear via the secondary facial foramen between the petrosal and epitympanic wing of the squamosal (Figures 2 and 7c). It runs posteriorly within the facial sulcus between the epitympanic recess and fenestra vestibuli, and then lateral to the stapedius fossa and across the stylomastoid notch at the base of the paroccipital process (Figures 5a and 7c) to exit the middle ear at the stylomastoid foramen (Figure 1).

Although the focus here is on the middle ear, I note unusual features on the endocranial surface of the petrosal regarding the subarcuate fossa, which houses the petrosal lobule of the cerebellum. As typical, the entrance into the subarcuate fossa is rimmed by the gyrus of the anterior semicircular canal (Figure 5b). Atypically, however, the petrosal does not completely floor the fossa and the bulk is formed by the squamosal (Figures 4a and 5b). There is a well-developed foramen in the floor of the fossa, the petromastoid canal (Gannon et al., 1988). It is nearly completely enclosed in the petrosal's contribution (Figure 4a) and connects to the posttemporal canal (Figure 5b), a longitudinal conduit between the petrosal and squamosal transmitting the arteria and vena diploëtica magna (Wible, 1993: figure 4C, D). Cartmill and MacPhee (1980) reported this canal in juvenile *Cynocephalus* crania, and Wible (1993) noted a vein here in "*Cynocelphalus*," DUCEC 839. Another unusual feature concerns the crista petrosa (Figures 4 and 6a). It arises anterior to the gyrus of the anterior semicircular canal, from which it is separated by a deep notch; it descends in height anteriorly and is not developed on the pars cochlearis anterior to the internal acoustic meatus.

The auditory bulla and osseous external acoustic meatus are shown in ventral and dorsal views in Figure 8. As observed by Klaauw (1922; see also Hunt & Korth, 1980; Wible & Martin, 1993), the bony bulla is composed of the intramembranous ectotympanic and two independent entotympanic elements (rostral and caudal) that preform in cartilage. There may also be a contribution from the ossified cartilage of the auditory tube (Wible & Martin, 1993). The ectotympanic is an open ring in prenatal stages, with two arms, the anterior and posterior crura, separated by a sizeable lateral gap, the tympanic incisure. The ectotympanic expands postnatally to be the primary element of the bulla and the osseous external acoustic meatus; the small entotympanics are situated along the dorsal rim of the ectotympanic in the anterior, medial, and posterior bullar margins. In AMNH 187861, the bony bulla has no indication of sutures delimiting the ectotympanic and entotympanics. Based on the work of the authors cited above, the ectotympanic is the sole element visible in the ventral view of the bulla (Figure 8a); however, it is unclear how much of the

entotympanics have ossified in the dorsal view (Figure 8b) as Wible and Martin (1993) found considerable cartilage in the postnatal DUCEC 806 and 839. There is an irregular area of bone in the anteromedial corner on the dorsal surface that differs from the otherwise smooth bony surfaces around it (Figures 5 and 8b); this is the only part that I am confident is entotympanic.

A defining feature on the dorsal (tympanic) surface of the bulla is the sulcus tympanicus (Figure 8b), the semicircular site of attachment of the tympanic membrane (tympanum). The disposition of the sulcus reveals that the tympanic membrane lies at a low angle to the horizontal, approximately 30°. The sulcus tympanicus separates the medially-placed middle ear from the laterally-placed external ear. The external ear is subdivided further into the recessus meatus, which is covered by the bulla proper, and the cylindrical external acoustic meatus. The bone flooring the recessus meatus has several small openings that likely result from the inflation of the ectotympanic; Kampen (1905) and Klaauw (1931) described similar openings in adults. In lateral view (Figure 7d), the opening of the meatus is roughly oval, taller than wide. Its smooth meatal roof is formed by the squamosal and its irregular sides and floor by the ectotympanic. Of the ectotympanic's contributions, that to the anterior wall is the most substantial (Figure 8a).

At the anterior margin of the bulla is a short, blunt styliform process (Figure 8), which is formed on the ectotympanic (Wible & Martin, 1993). Dorsal to the styliform process is a broad channel for the auditory tube that is bordered posteriorly by the entotympanic (Figure 8b). Based on *C. volans*, DUCEC 806, this channel is transformed into a large aperture by the U-shaped cartilage of the auditory tube (see its bullar attachments in Figure 8b), which as noted above underlies the epitympanic wing of the petrosal. The cartilage of the auditory tube bridges the small gap between the entotympanic and epitympanic wing visible in Figure 7d.

Of the neighboring basicranial bones, the bulla and osseous external acoustic meatus only have direct contacts with the petrosal and squamosal. The petrosal contacts are on the caudal tympanic and paroccipital processes, the latter being partially fused and including a small canal transmitting the chorda tympani nerve into the middle ear (Figure 8b). The squamosal contacts are on the epitympanic wing, postglenoid process, and posttympanic process, the last two being partially fused to the osseous meatus.

A final structure on the bulla concerns the Glaserian fissure, which developmentally is the conduit for Meckel's cartilage and with that element's disappearance in later ontogenetic stages contains the chorda tympani nerve (Klaauw, 1931). In the prenatal specimens (*C. volans*, DUCEC 804, and "*Cynocephalus*," DUCEC 8310), Meckel's cartilage runs forward from the developing incus and malleus in company with the gonial bone and chorda tympani nerve, as typical for mammals (De Beer, 1937). The cartilage and nerve in DUCEC 804 and 8310 cross the anterior crus (arm) of the ring-like ectotympanic, but the gonial does not reach as far anteriorly. Unfortunately, these structures are not well preserved in the postnatal specimens (DUCEC 806 and 839), so their fate is uncertain. AMNH 187861 has a thread-like anterior process of the malleus (likely formed from the gonial of the prenatal specimens) that at its distal tip sits in a groove on the ectotympanic part of the bulla (Figures 7d and 8b), the groove representing the Glaserian fissure. The groove, which is longer than the anterior process of the malleus, also contained the chorda tympani nerve. Anteroventral to the Glaserian fissure, there is a seam in the bulla that ends at a short spine (Figure 6d). The meaning of this seam and spine is unknown.

The middle-ear ossicles are shown in situ in the basicranium in Figure 2, and on the isolated petrosal in Figures 6c and 7b,d. The malleus (Figure 9a–c) has an anteroposteriorly compressed head with two incudal articular facets set at approximately 145° to each other. The larger superior facet is concave and the inferior facet convex. Anterior to the head is a small, triangular osseous lamina that tapers into a thread-like anterior process. As segmented here, a tiny gap separates the anterior process (i.e., gonial bone) from the osseous lamina. This gap does not appear to be a thresholding issue but was likely filled with cartilage connecting the two bones. A short neck connects the head to the manubrial base. The neck has a tiny muscular process for the attachment of the tensor tympani muscle. Based on *C. volans*, DUCEC 804, the chorda tympani nerve crosses the malleus ventral to the muscular process (epitensoric position) as previously reported in a juvenile *C. volans* by Maier (2008). The manubrial base has a prominent lateral process to which the upper part of the tympanic membrane is attached. The manubrium is anteroposteriorly compressed with a ridge along its posterolateral aspect and an expanded tip.

The incus (Figure 10a–c) has a prominent, rounded body that is larger than the head of the malleus. There are two mallear articular facets; the larger inferior facet is concave and the superior relatively flat. The short process, crus breve, is remarkably short when compared to the long process, crus longum. There is a distinct lenticular process articulating with the stapes that is separated from the crus longum by a sizeable gap. This gap was likely filled with cartilage during life. The prenatal specimens, *C. volans*, DUCEC 804, and "*Cynocelphalus*," DUCEC 8310, have an incus preformed in cartilage that has continuity between the lenticular process and crus longum.

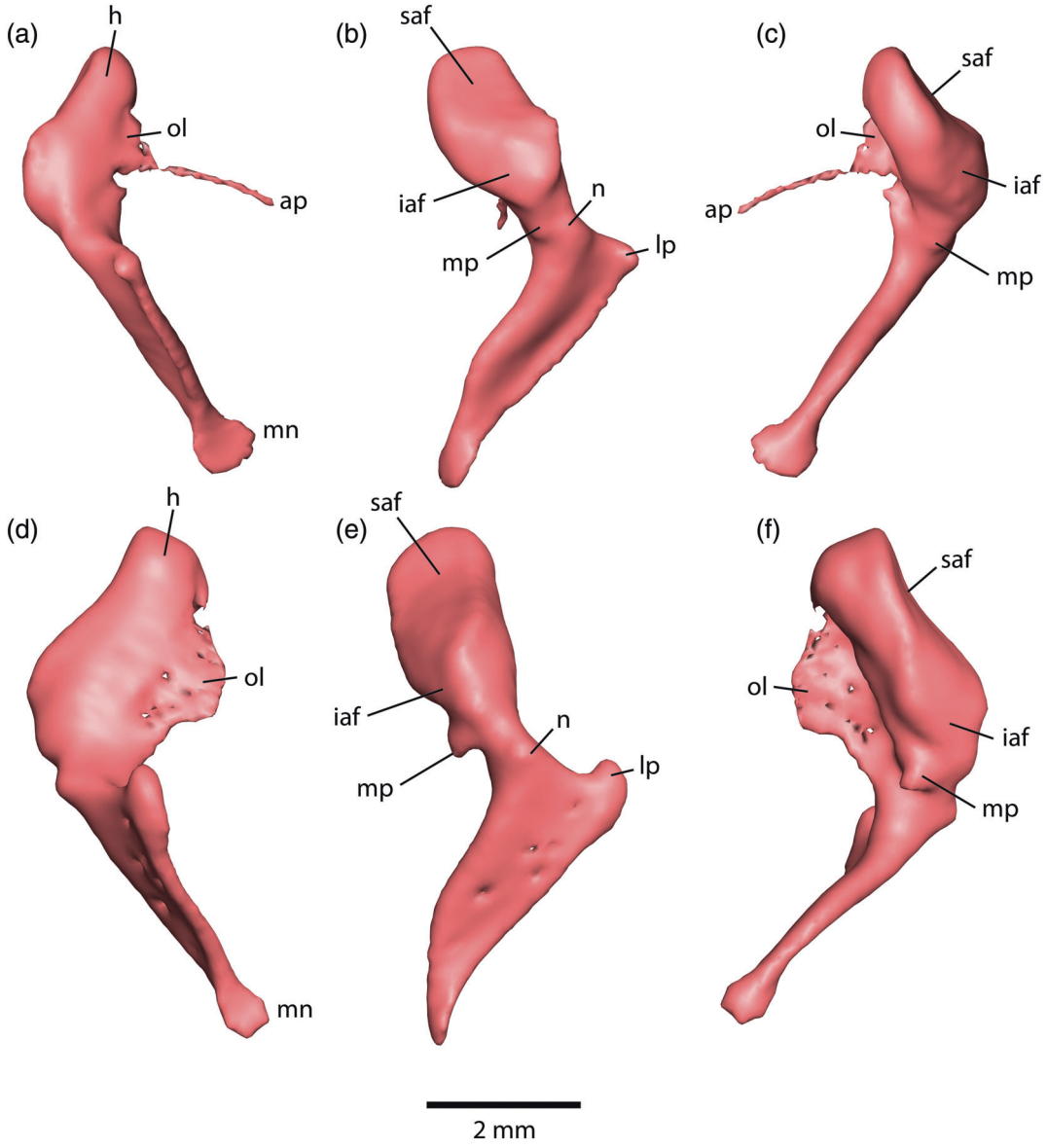

FIGURE 9 *Cynocephalus volans*, isosurfaces derived from the CT scans of the right malleus. (a–c) AMNH 187861; (d–f) FMNH 56442. (a, d) Oblique lateral view; (b, e) oblique posterior view; (c, f) oblique medial view. Abbreviations: ap, anterior process; h, head; iaf, inferior articular surface; lp, lateral process; mn, manubrium; mp, muscular process; n, neck; ol, osseous lamina; saf, superior articular surface.

The stapes (Figure 11) has a head that is broader than the lenticular process and with no indication of a muscular process for the attachment of the stapedius muscle, a muscle known to be present from the histological specimens. The two crura border an oval stapedial foramen, taller than wide. The anterior crus is thinner and more bowed than the posterior crus. The posterior crus is expanded at both the head and the footplate, although significantly more at the latter. The footplate is slightly longer than the stapes is tall and has a stapedial ratio (length/width) of 1.65, whereas as noted above the fenestra vestibuli is 1.60. The footplate is bulbous on the surface facing the inner ear and concave between the crura.

3.2 | *Cynocephalus volans*, FMNH 56442

Description of the cranium of this adult female is complicated by the near total absence of sutures delimiting bones (Figure 12). The petrosal is the only bone that is somewhat distinguished by sutures (Figure 13), although much of the pars canalicularis is fused to the squamosal, exoccipital, and auditory bulla. In the following, attention is given to the major differences between the juvenile, AMNH 187861, and the adult, FMNH 56442.

An obvious difference is the lack of indication of the parasphenoid bone on the basisphenoid, which is clear on the juvenile (Figure 1); it is uncertain if this bone's presence is polymorphic or if it is wholly subsumed by

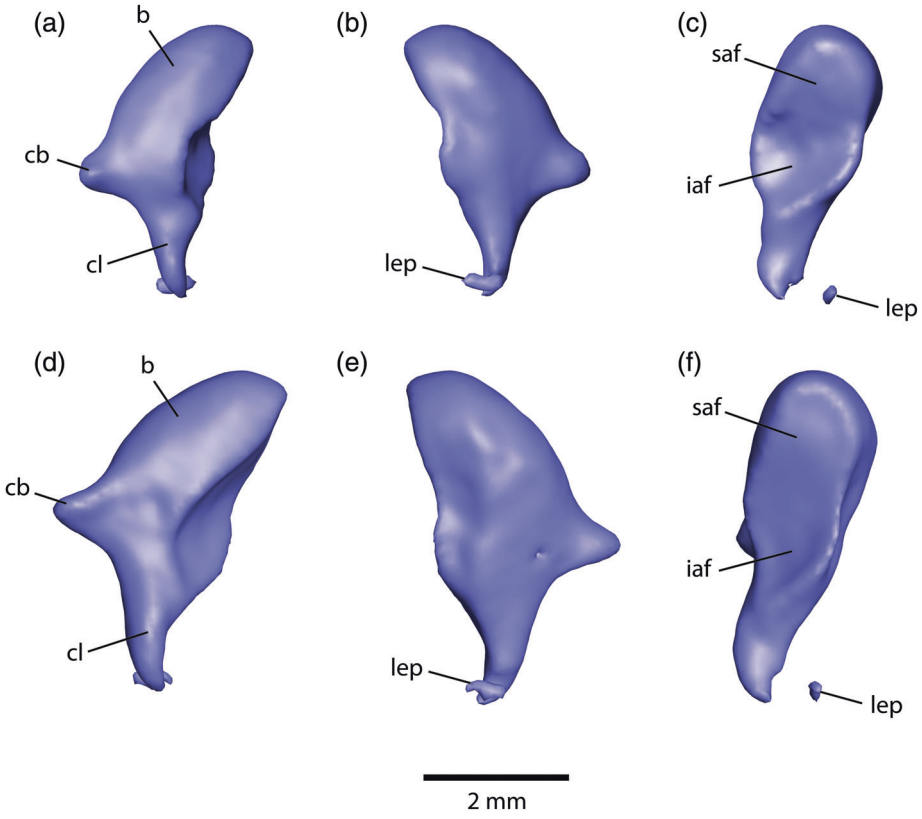

FIGURE 10 *Cynocephalus volans*, isosurfaces derived from the CT scans of the right incus. (a–c) AMNH 187861; (d–f) FMNH 56442. (a, d) Oblique lateral view; (b, e) oblique posterior view; (c, f) oblique medial view. Abbreviations: b, body; cb, crus breve; cl, crus longum; iaf, inferior articular surface; lep, lenticular process; saf, superior articular surface.

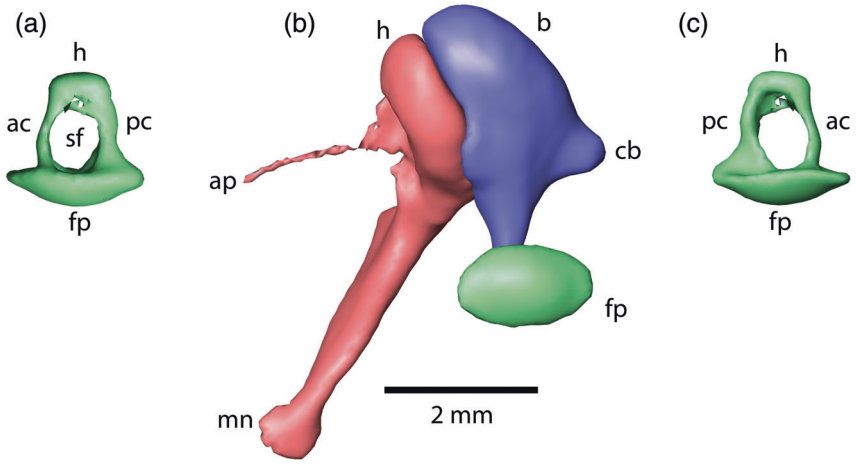

FIGURE 11 *Cynocephalus volans*, AMNH 187861, isosurfaces derived from the CT scans of the right middle ear ossicles. (a) Stapes in oblique dorsal view; (b) malleus, incus, and stapes in oblique medial view; (c) stapes in oblique ventral view. Abbreviations: ac, anterior crus; ap, anterior process; b, body; cb, crus breve; fp, footplate; h, head; mn, manubrium; pc, posterior crus; sf, stapedial foramen.

the basisphenoid. Compared to the juvenile, the auditory bulla and osseous external acoustic meatus are greatly expanded in the adult (cf. Figures 1 and 12), which creates several new openings detailed below. The mastoid is also more inflated, via its continuity with the epitympanic sinus of the squamosal. The expanded bulla contacts and fuses to bones that it does not contact in the juvenile, namely the basioccipital medially, the exoccipital posteromedially, and the basisphenoid, alisphenoid, and squamosal anteriorly; the bulla also abuts the outer edges of the pars cochlearis. It is unclear which element(s) of the bulla (i.e., ectotympanic, entotympanic, and ossified cartilage of the auditory tube) account for the expansion present in the adult. As in the juvenile, the floor of the recessus meatus has several openings in it (as also reported by Kampen, 1905 and Klaauw, 1931), but these are smaller.

Along the anterior aspect of the bulla, the juvenile has an insignificant styliform process on the ectotympanic (Figure 8), whereas this is elongate in the adult (Figure 12). Dorsal to the styliform process, the juvenile has a broad gap that includes the auditory tube and its cartilage (Figure 8b). In the adult, bone fills this gap, presumably derived from the entotympanic and/or cartilage of the auditory tube (Wible & Martin, 1993).

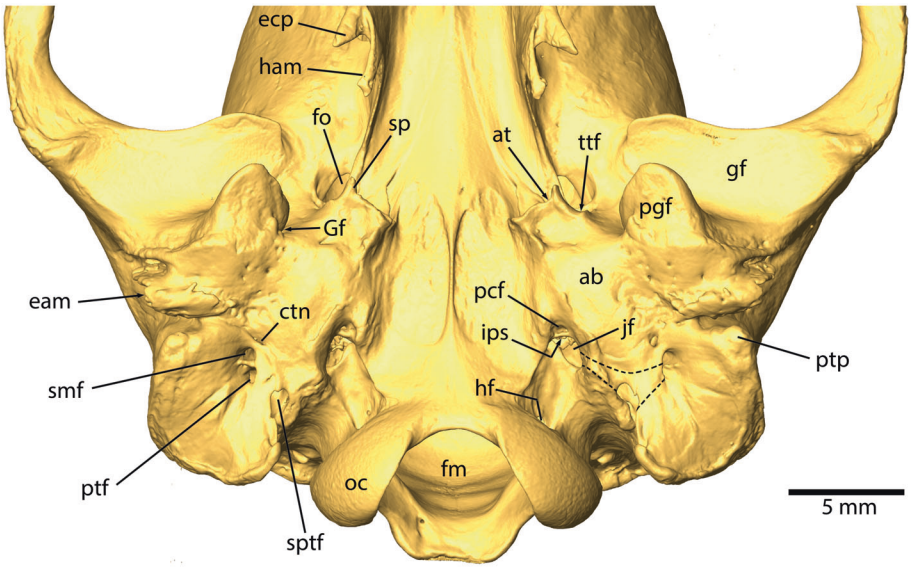

FIGURE 12 *Cynocephalus volans*, FMNH 56442, isosurface derived from the CT scans of the basicranium in ventral view. Dashed lines indicate canal connecting the jugular, posttemporal, and secondary posttemporal foramina. Abbreviations: ab, auditory bulla; at, to auditory tube opening; ctn, for chorda tympani nerve; eam, external acoustic meatus; ecp, ectopterygoid process; fm, foramen magnum; fo, foramen ovale; gf, glenoid fossa; Gf, Glaserian fissure; ham, pterygoid hamulus; hf, hypoglossal foramen; ips, to inferior petrosal sinus opening; jf, jugular foramen; oc, occipital condyle; pcf, posterior carotid foramen; pgp, postglenoid process; ptf, posttemporal foramen; ptp, posttympanic process; ptc, posttemporal foramen; smf, stylomastoid foramen; sp, styliform process; sptf, secondary posttemporal foramen; ttf, to opening into tensor tympani fossa.

FIGURE 13 *Cynocephalus volans*, FMNH 56442, isosurface derived from the CT scans of the right endocranium in oblique medial view. Right petrosal is in light blue. Abbreviations: ccf, caudal cranial fossa; cevs, capsuloparietal emissary vein sulcus; ci, to carotid incisure; cs, cavum supracochleares; fai, foramen acusticum inferius; fas, foramen acusticum superius; fm, foramen magnum; fo, foramen ovale; ham, pterygoid hamulus; hf, hypoglossal foramen; hyf, hypophyseal fossa; ips, inferior petrosal sinus opening; jf, jugular foramen; mcf, middle cranial fossa; mg, meningeal groove; of, optic foramen; pf, piriform fenestra; pmc, petromastoid canal; ptc, posttemporal canal; ptg, posttemporal groove; saf, subarcuate fossa; scs, sinus communicans sulcus; sof, sphenorbital fissure; sss, sigmoid sinus sulcus; tg, trigeminal groove.

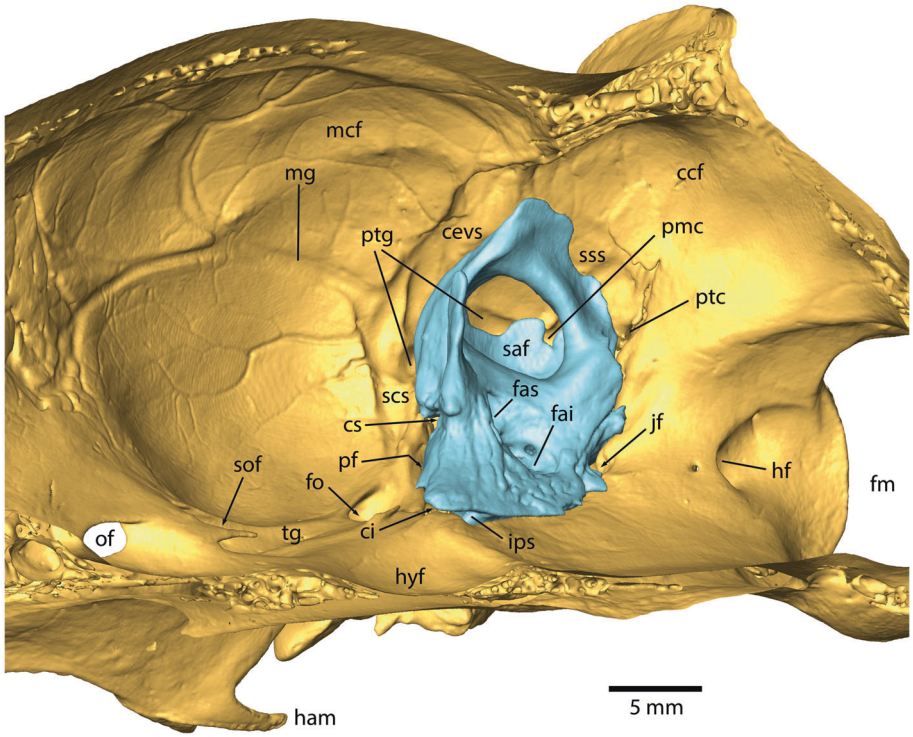

Two bony conduits into the middle ear are delimited (not visible but indicated by arrows in Figure 12): a larger medial aperture for the auditory tube and a smaller lateral one that leads into the fossa for the tensor tympani muscle. Based on *C. volans*, DUCEC 806, this aperture transmits the nerve to the tensor tympani and the anterior tympanic artery, a branch of the maxillary artery (Wible, 1993). It is unknown if any tubal cartilage remains in the adult or if it is entirely replaced with bone.

The osseous external acoustic meatus has a more complete floor in the adult, but its composition remains as in the juvenile with a smooth roof formed by the squamosal and walls showing a layer of irregular bone formed by the ectotympanic. The ends of the anterior and posterior crura are solidly fused to the medial margin of the squamosal roof of the osseous meatus, but there is no indication of ectotympanic growth between the crural ends. Consequently, a large tympanic incisure is present in the adult as in the juvenile.

The main openings at the posteromedial (jugular foramen) and posterolateral (stylomastoid and posttemporal foramina) aspects of the ear region in FMNH 56442 are as in the juvenile AMNH 187861 (cf. Figures 1 and 12). Two differences posteromedially are that the adult also has a foramen for the inferior petrosal sinus and a posterior carotid foramen (Figure 12). The former is anterior to the jugular foramen and leads anteriorly into a canal between the bulla (likely entotympanic portion), basioccipital (based on position), and petrosal. The latter, for the internal carotid nerves (Wible, 1993), is in a small depression ventral to the foramen for the inferior petrosal sinus and leads into a short canal through the bulla that opens onto the promontorium. As the juvenile has a broad gap between the pars cochlearis and bulla where the internal carotid nerves enter the middle ear, it is likely that the posterior carotid foramen in the adult is entirely in the entotympanic. Another unusual feature posteromedially in the adult is a broad channel connecting the jugular and hypoglossal foramina, presumably transmitting a vein connecting the internal jugular and posterior meningeal veins (Wible, 1993). Posterolaterally, the small foramen for the chorda tympani nerve is visible in direct ventral view in the adult, but is hidden in the same view in the juvenile.

A major difference between the adult and juvenile is the presence in the former of an opening in the mastoid area ("sptf" in Figure 12) roughly equidistant to the jugular and posttemporal foramina that is wholly lacking in the juvenile (Figure 1). This opening first was reported in *C. volans* by Hunt and Korth (1980). They identified this foramen as between the exoccipital and mastoid, and proposed it as a mastoid venous foramen (see also Cartmill & MacPhee, 1980; MacPhee et al., 1989). However, Wible (1993) showed that the occupants of this foramen are arterial and venous, the arteria and vena diploëtica magna, branches of the occipital artery and vein. Although Wible (1993) showed the term "mastoid venous foramen" to be inappropriate, he did not offer an alternative.

Study of the CT scans of FMNH 56442 (and in the context of AMNH 187861) reveals more detail about the anatomy here. As suggested by Hunt and Korth (1980), the exoccipital and mastoid are contributing elements to the foramen; the former forms the medial border and the mastoid (caudal tympanic process) the roof. However, the floor of the foramen appears to be formed by posterior growth of the bulla, although it is uncertain whether this is through expansion of the ectotympanic, entotympanic, or both. The true nature of the floor composition requires a specimen bridging the condition of no foramen in AMNH 187861 (Figure 1) and the enclosed foramen in FMNH 56442 (Figure 12). The foramen in the latter leads into a broad canal, the contours of which are indicated in Figure 12 by dashed lines on the left side of FMNH 56442; this canal is stretched between the jugular and posttemporal foramina. The main occupants of the larger lateral stretch of the canal are, following Wible (1993), the arteria and vena diploëtica magna. This lateral canal transmits the artery and vein to the posttemporal foramen. In light of the occupants and later ontogenetic formation of the foramen into the lateral canal, the term "secondary posttemporal foramen" seems an appropriate moniker. The smaller medial stretch of the canal to the jugular foramen likely transmits the auricular branch of the vagus nerve, which continues into the lateral stretch of the canal to ultimately reach the facial nerve at the stylomastoid foramen.

The endocranial aspect of the petrosal is fully delimited by sutures from its neighbors (Figure 13). However, growth around the edges of the petrosal largely closes off the gaps present along the anterior and medial edges in the juvenile (Figure 4a). The broad basicapsular fissure of the juvenile is largely enclosed into a canal for the inferior petrosal sinus with the petrosal growing over the basioccipital except at the anteromedial corner where there is an entrance to the canal (Figure 13). The carotid incisure is present although reduced to mere sliver and no longer easily visible in the endocranial view. The petrosal is still separated from the epitympanic wing of the squamosal by a tiny gap, but it is not enough to identify this as a piriform fenestra. The cavum supracochleare remains a depression in the anterior surface of the petrosal, and not enclosed in that bone, and the entrance of the facial nerve into the middle ear, the secondary facial foramen, lies between the petrosal and squamosal (not visible in Figure 13). As in the juvenile, the petrosal does not completely floor the subarcuate fossa. The crista petrosa is as in the juvenile, separated from the gyrus of the anterior semicircular canal by a deep notch and not developed on the anterior half of the pars cochlearis. A remarkable change from the juvenile to the adult concerns the enlargement and addition of grooves related to the vascular system. For example, the juvenile has a small sulcus for the sinus communicans anterior to the petrosal in the middle cranial fossa (Figure 4a), but this is dramatically larger in the adult (Figure 13).

Within the middle ear, the cochlea is coiled 940°, whereas it is 954° as reported by Ekdale (2013) and 945° in the juvenile, AMNH 187861. The stapedial ratio (length to width of the oval window) is 1.65, whereas it is 1.60 in AMNH 187861. The faint grooves for the internal carotid nerves on the promontorium in the juvenile (Figure 6a) are present but even fainter in the adult. The disposition of the sulcus tympanicus shows the tympanum to be at a slightly lower angle to the horizontal in the adult compared to the juvenile, 25° versus 30°. Only the left malleus and incus are preserved in FMNH 56442. Both bones (Figures 9d–f and 10d–f) resemble those described for the juvenile (Figures 9a–c and 10a–c) but are more robust. The adult malleus has more prominent muscular and lateral processes and osseous lamina. The adult incus has more robust short and long processes and body. A major difference is the total lack of the anterior process of the malleus, which is thread-like in the juvenile. A striking similarity is the absence of bone connecting the lenticular process to the long process of the incus. The CT scans show an unossified structure connecting the two, which presumably is cartilaginous.

4 | DISCUSSION

Study of the CT scans of the juvenile and adult *C. volans* has uncovered some novel observations as well as some discrepancies with prior observations in the literature that are addressed here.

4.1 | Subarcuate fossa

Although a petromastoid canal has been reported previously for *C. volans* (Cartmill & MacPhee, 1980; O'Leary et al., 2013: morphobank project 773), the observation here that the petrosal's contribution to the floor of the fossa is incomplete and supplemented by squamosal in the juvenile AMNH 187861 and adult FMNH 56442 (Figures 4 and 13) is novel. Given how seldom the endocranial surface of the petrosal is studied or illustrated, I am uncertain how unusual this arrangement is in mammals. I reported a similar arrangement in the pen-tailed treeshrew *Ptilocercus lowii*, where the parietal and not the squamosal completed the subarcuate fossa floor (Wible, 2011). In the prenatal sectioned specimens studied here, *C. volans*, DUCEC 804, and "*Cynocephalus*," DUCEC 8310, and in the 28- and 63-mm crown-rump length *C. volans* embryos described by Henckel (1929) and Halbsguth (1973), respectively, the cartilaginous pars canalicularis forms the entire subarcuate fossa. In the smaller postnatal sectioned specimen, *C. volans*, DUCEC 806, the ossified pars canalicularis also is complete within the subarcuate fossa. However, the larger postnatal sectioned specimen, "*Cynocephalus*," DUCEC 836, has the same condition as in AMNH 187861 and FMNH 56442. This change in DUCEC 836 precedes the considerable pneumatization of the petrosal found in the adult and to a lesser extent in the juvenile.

4.2 | Posterior carotid foramen

A complete internal carotid artery is lacking in the prenatal colugo specimens studied by Wible (1993). However, in light of what we know about the development of this artery in mammals (e.g., Presley, 1979; Wible, 1986), a complete vessel was likely present in early embryos of *C. volans*. The internal carotid nerves follow the course of the artery and were left on the promontorium with the involution of the transpromontorial segment of the artery. The existence of a posterior carotid foramen in the adult bulla by which the nerves reach the promontorium is debated. Hunt and Korth (1980: p. 178) wrote "In dried adult skulls, no foramina for entrance of the internal carotid into the auditory area are identifiable, either in the basicranial bones or in the bulla itself." Wible (1993: figure 6) showed that the internal carotid nerves enter the middle ear near the jugular foramen in *C. volans*, DUCEC 806, but did not describe or illustrate this opening in the adult. A posterior carotid foramen in the posteromedial bullar wall was scored as present in O'Leary et al. (2013: morphobank.org project 773). Yet, to my knowledge, this opening has not been identified in the adult colugo in any figures in the literature. Consequently, the labelling of the posterior carotid foramen in FMNH 56442 (Figure 12) rectifies this. Revisiting photos of *C. volans* already published, the posterior carotid foramen is visible near the posterior lacerate foramen (= jugular foramen) in Hunt and Korth (1980: figure 9) and MacPhee et al. (1989: figure 8a).

4.3 | Tympanic incisure

Hunt and Korth (1980: pp. 177–178) wrote "We conclude that the dermopteran bulla is in composition and orientation simply a primitive eutherian bulla, but with one striking modification: closure of the tympanic crescent by ossification between the crura resulting in enclosure of the eardrum within the bulla." Their figure 15 showed part of the bulla removed from a neonate, FMNH 56782, with the following note in the figure legend: "Note that the meatal aperture of the tympanic bone is a complete tube closed dorsad that transmits sound waves into the

recessus meatus." Their figure 3 showed this diagrammatically in the adult, with the ectotympanic forming the roof of the osseous external acoustic meatus. Extrapolating from these observations, Hunt and Korth (1980) are reporting the absence of a tympanic incisure between the ectotympanic crura, which was followed for this taxon in the phylogenetic analysis of O'Leary et al. (2013: morphobank.org project 773).

In the juvenile AMNH 187861, an osseous tubular external acoustic meatus is present, but it is not formed entirely by the ectotympanic, in contrast to the observations of Hunt and Korth (1980). The anterior and posterior walls show a double layer with the inner irregular surface formed by the ectotympanic, which also forms the floor; the roof has a single smooth layer formed by the squamosal. A large tympanic incisure separates the anterior and posterior crura (Figure 8). The adult, FMNH 56442, shows the same pattern, albeit with more fusion between the structures.

In light of these new observations, the specimen studied by Hunt and Korth (1980) should be revisited to see if *C. volans* is polymorphic for the presence/absence of a tympanic incisure.

4.4 | Middle-ear ossicles

Colugo middle-ear ossicles have been studied and illustrated by Doran (1878), Parker (1885), and Fleischer (1973). The most detailed of these is Parker (1885), which includes a "ripe embryo" 5.5 in. from snout to base of tail of *Galeopithecus volans* and an adult *Galeopithecus philippensis* (both of which = *C. volans*). In Parker's embryo (Figure 14a), the ossicles are ossified except the mallear/incudal articular surfaces. Parker (1885) described the malleus as having a slender processus gracilis (= anterior process) and a bulbous head, although the latter does not appear to be much different from the head of AMNH 187861 and FMNH 56442 (Figure 9), which I consider to be anteroposteriorly compressed. In Parker's adult (Figure 14b), the anterior process is essentially gone. He did not report a muscular process on the malleus in either stage, which differs from the specimens here (Figure 9). The incus of Parker's adult (Figure 14b) generally resembles those of AMNH 187861 and FMNH 56442 (Figure 10), whereas that of the 5.5 in. embryo has a less bulbous body and more elongate crus breve (Figure 14a). Without comment, Parker (1885) illustrated the incus of the 5.5 in. embryo without a lenticular process and with a ligament connecting the crus longum to the stapes (Figure 14a). He pictured a lenticular process on the adult incus (Figure 14b), and as he made no comment on it, I presume it is continuous with the crus longum, unlike the incudes studied here (Figure 10). The stapes of Parker's adult (Figure 14b) resembles that of AMNH 187861 (Figure 11), but differs in having a distinct muscular process for the insertion of the stapedius muscle and an ossified interhyal (= cartilage of Paaw) in the stapedius muscle tendon. As discussed by Wible and Shelley (2021), the incidence of the cartilage of Paaw may be affected by preparation techniques, so that its occurrence in AMNH 187861 should be considered unknown. The stapes of

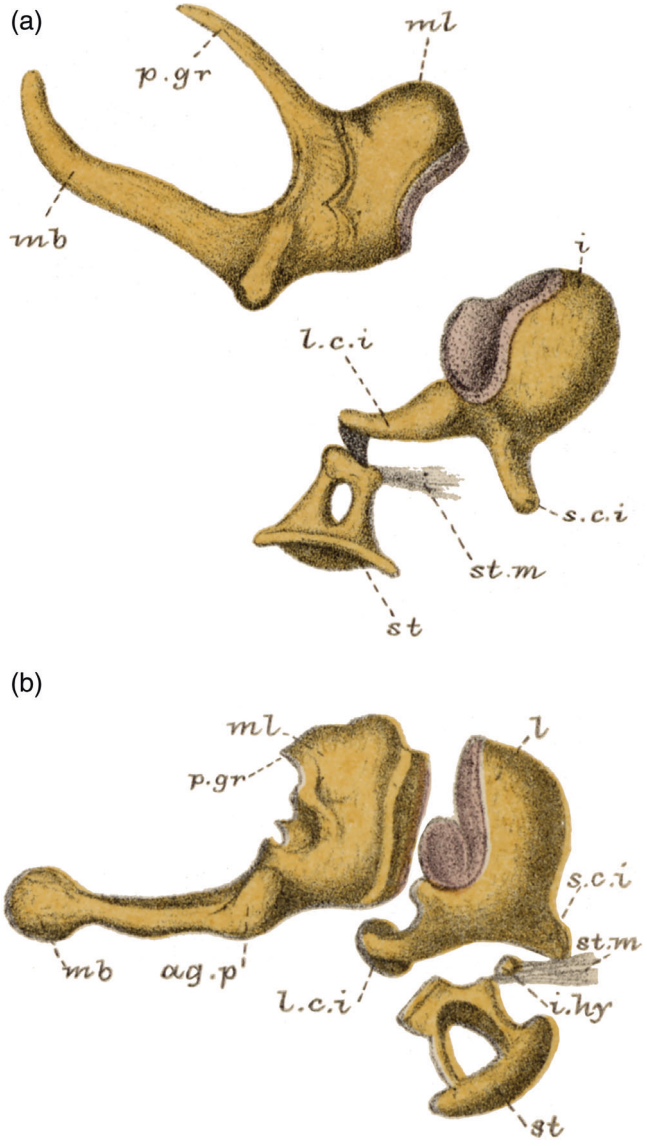

FIGURE 14 *Cynocelphalus volans*, middle-ear ossicles in outer view. (a) *Galeopithecus volans*, 5.5 in. embryo, from Parker (1885: plate 37, figure 4); (b) *Galeopithecus philippinensis*, adult, from Parker (1885: plate 39, figure 3). Bone is yellow, cartilage red. Abbreviations (Parker's original with synonyms as needed): ag.p, posterior angular process (lateral process); i, incus; i.hy, interhyal (cartilage of Paaw); l.c.i, long crus of incus (crus longum); mb, manubrium; ml, malleus; p.gr, processus gracilis (anterior process); s.c.i, short crus of incus (crus breve); st, stapes; st.m, stapedius muscle.

Parker's 5.5 in. embryo (Figure 14a) differs from that of AMNH 187861 (Figure 11) in having a much smaller stapedial foramen.

Doran (1878) noted a tubular muscular process and a slender processus gracilis (= anterior process) on the malleus in adult *Galeopithecus*, but the latter is not included in his illustration (plate LXII, figure 18). He reported the Sylvian apophysis (= lenticular process) continuous with the crus longum of the incus. Fleischer (1973) studied three *Cynocephalus variopedatus*, which he equated with *Galeopithecus volans* (= *C. volans* here). The most significant differences in the descriptions and illustration in Fleischer (1973) compared to the specimens here concern the malleus; his adult is illustrated with a slender processus gracilis (= anterior process) resembling that in the 5.5 in. embryo of Parker (1885) although thinner and he reported the muscular process as absent.

These few descriptions and illustrations highlight a significant level of variability in the middle-ear ossicles. Is it possible that the taxonomy in these older works is questionable? Or are these differences polymorphisms within *C. volans*? Additional observations are needed to address this.

In the history of human anatomical studies, the lenticular process has been considered to be a fourth middle-ear ossicle (os lenticulare), as the thin pedicle connecting the process to the crus longum was not always readily detected in early anatomical preparations (Graboyes et al., 2011). Today, it is generally held that the lenticular process is part of the human incus (e.g., Strandring, 2008). Nevertheless, instances in humans where there is no connection or the lenticular process is absent are reported. Chien et al. (2009) found no connection in histological preparations of 9 of 270 human incudes studied. Lannigan et al. (1993) found increased osteoclastic activity to the lenticular process and adjacent crus longum with advancing age in humans, including the total erosion of the lenticular process. How do these studies inform the situation of the incus in AMNH 187861 and FMNH 56442 (Figure 10)? Above, I speculated that cartilage breeched the gap between the crus longum and lenticular process in both, with continuous cartilage present in the prenatal DUCEC 804 and 8310. Unfortunately, the incus is not well preserved in the postnatal DUCEC 806 and 839, which might have provided information to address this issue. Until more data are forthcoming, the meaning of the bony gap in the colugo incus is unknown.

4.5 | Posttemporal foramen and canal

The arteria and vena diploëtica magna are found in extant monotremes and some extant marsupials and placentals (Rougier & Wible, 2006; Wible, 1987, 2003), including colugos (Wible, 1993). The posttemporal foramen and canal, which transmit these vessels in extant mammals, are widely distributed among Mesozoic mammaliaforms, including Late Cretaceous eutherians (Wible et al., 2004, 2009). To date, the colugos, *C. volans* and *Galeopterus variegatus*, are the only taxa, extant or extinct, reported with a posttemporal foramen within Euarchontoglires, the broader clade that includes Dermoptera, Primates, Scandentia, Rodentia, and Lagomorpha (O'Leary et al., 2013: morphobank.org project 774). The presence of these vessels in colugos with their highly derived vascular system and ear region among Euarchontoglires is an unexpected distribution. The posttemporal foramen in *C. volans* (Figures 1, 2, and 12) and *Galeopterus variegatus*, CM 87908, 87909 (pers. obs.), differs from that in all other mammals in having a posttemporal foramen that it is not on the occiput but on the basicranium. Additionally, the colugos are further distinguished by having a secondary posttemporal foramen that leads to the primary (Figure 12).

4.6 | Comparisons with other taxa

The ultimate goal of this research is to make comparisons with other taxa for the purposes of phylogenetic reconstruction and functional interpretations. To achieve those ends, a first step is to conduct similar studies on the other living dermopteran, the Sunda flying lemur, *Galeopterus variegatus*. Given that their adult crania are similarly devoid of most sutures, studies of juveniles will also be required. Until such studies are forthcoming, comparisons are premature if the goal is to identify features of the ear region related to gliding locomotion versus those related to the broader phylogenetic relations of dermopterans.

AUTHOR CONTRIBUTIONS

John R. Wible: Conceptualization; investigation; funding acquisition; writing – original draft; methodology; validation; visualization; writing – review and editing; data curation; project administration; software; formal analysis; supervision; resources.

ACKNOWLEDGMENTS

I thank the organizers of this special issue, Tim D. Smith and Valerie B. DeLeon, for the invitation to submit an article in celebration of Kunwar P. Bhatnagar. I had the privilege of being in the Department of Anatomical Sciences and Neurobiology at the University of Louisville School of Medicine from 1989 to 1998 with my colleague and friend Kunwar. We shared many interests, primarily related to bats and the vomeronasal organ, and coauthored seven

papers together. Kunwar was always interested and supportive of my many other interests as well, including projects on the basicranial anatomy of the colugo (Wible, 1993; Wible & Martin, 1993). It is fitting that a follow-up to that research is my contribution to his memorial.

I thank Doug Boyer, Duke University, and MorphoSource.org along with the American Museum of Natural History and Field Museum of Natural History for access to CT scans. Paul Bowden, Carnegie Museum of Natural History, added the facial nerve to Figure 7c and dashed lines to Figure 12. This report benefitted considerably from the comments of Mary Silcox and an anonymous reviewer. Funding for this project is from National Science Foundation Grant DEB 1654949.

CONFLICT OF INTEREST STATEMENT

The author declares no conflicts of interest.

DATA AVAILABILITY STATEMENT

All data are included here.

ORCID

John R. Wible https://orcid.org/0000-0002-0721-1228

REFERENCES

Álvarez-Carretero, S., Tamuri, A. U., Battini, M., Nascimento, F. F., Carlisle, E., Asher, R. J., Yang, Z., Donoghue, P. C. J., & Dos Reis, M. (2022). A species-level timeline of mammal evolution integrating phylogenomic data. *Nature*, *602*, 263–267.

Audebert, J. B. (1799). *Histoire naturelle des singes Makis*. Desray.

Cartmill, M., & MacPhee, R. D. E. (1980). Tupaiid affinities: The evidence of the carotid arteries and cranial skeleton. In W. P. Luckett (Ed.), *Comparative biology and evolutionary relationships of tree shrews* (pp. 95–132). Plenum Press.

Chien, W., Northrop, C., Levine, S., Pilch, B. Z., Peake, W. T., Rosowski, J. J., & Merchant, S. N. (2009). Anatomy of the distal incus in humans. *Journal of the Association for Research in Otolaryngology*, *10*, 485–496.

De Beer, G. R. (1937). *The development of the vertebrate skull*. Clarendon Press.

Diogo, R. (2009). The head and neck muscles of the Philippine colugo (Dermoptera: *Cynocephalus volans*), with a comparison to tree-shrews, primates, and other mammals. *Journal of Morphology*, *270*, 14–51.

Doran, A. H. G. (1878). Morphology of mammalian ossicula auditûs. *Transactions of the Linnean Society of London, 2nd Series. Zoology*, *1*, 391–497.

Ekdale, E. K. (2013). Comparative anatomy of the bony labyrinth (inner ear) of placental mammals. *PLoS One*, *8*(6), e66624.

Fleischer, G. (1973). Studien am Skelett des Gehörorgans der Säugetiere, einschließlich des Menschen. *Saugetierkundliche Mitteilungen*, *21*, 131–239.

Gannon, P. J., Eden, A. R., & Laitman, J. T. (1988). The subarcuate fossa and cerebellum of extant primates: Comparative study of a skull-brain interface. *American Journal of Physical Anthropology*, *77*, 143–164.

Gaupp, E. (1905). Neue Deutungen auf dem Gebiete der Lehre vom Säugetierschädel. *Anatomischer Anzeiger*, *27*, 272–310.

Graboyes, E. M., Hullar, T. E., & Chole, R. A. (2011). The lenticular process of the incus. *Otology & Neurotology*, *32*, 1600–1604.

Halbsguth, A. (1973). Das Cranium eines Foeten des Flattermaki *Cynocephalus volans* (*Galeopithecus volans*) (Mammalia. Dermoptera) von 63 mm SchStlg. In *Inaug. Diss. Med. Frankfurt Am Main* (p. 96).

Henckel, K. (1929). Die Entwicklung des Schädels von *Galeopithecus temmincki* Waterh. und ihre Bedeutung fur die stammesgeschichtliche und systematische Stellung der Galeopithecidae. *Morphologisches Jahrbuch*, *62*, 179–205.

Henson, O. W., Jr. (1961). Some morphological and functional aspects of certain structures of the middle ear in bats and insectivores. *University of Kansas Science Bulletin*, *41*, 151–255.

Hunt, R. M., Jr., & Korth, W. W. (1980). The auditory region of Dermoptera: Morphology and function compared to other living mammals. *Journal of Morphology*, *164*, 167–211.

Kampen, P. N. van (1905). Die Tympanalgegend des Säugetierschädels. *Morphologisches Jahrbuch*, *34*, 321–722.

Klaauw, C. J. van der (1922). Uber die Entwickelung des Entotympanicums. *Tijdschrift der Nederlandsche Dierkundige Vereeniging*, *18*, 135–174.

Klaauw, C. J. van der (1931). The auditory bulla in some fossil mammals with a general introduction to this region of the skull. *Bulletin of the American Museum of Natural History*, *62*, 1–352.

Lannigan, F. J., O'Higgins, P., & McPhie, P. (1993). Remodelling of the normal incus. *Clinical Otolaryngology*, *18*, 155–160.

Leche, W. (1886). Über die Säugethiergattung *Galeopithecus*: Eine morphologische Untersuchung. *Kungliga Svenska Vetenskapsakademiens Handlingar*, *21*, 3–92.

Linnaeus, C. (1758). *Systema Naturae per regna tria naturae, secundum classis, ordines, genera, species cum characteribus, differentiis, synonymis, locis* (Editio Decima ed., Reformata. Tomus I). Laurentii Salvii.

MacIntyre, G. T. (1972). The trisulcate petrosal pattern of mammals. In T. Dobzhansky, M. K. Hecht, & M. C. Steere (Eds.), *Evolutionary biology* (Vol. 6, pp. 275–303). Appleton-Century-Crofts.

MacPhee, R. D. E., Cartmill, M., & Rose, K. D. (1989). Craniodental morphology and relationships of the supposed Eocene dermopteran *Plagiomene* (Mammalia). *Journal of Vertebrate Paleontology*, *9*, 329–349.

Maier, W. (2008). Epitensoric position of the chorda tympani in Anthropoidea: A new synapomorphic character, with remarks on the fissura Glaseri in primates. In E. J. Sargis & M. Dagasto (Eds.), *Mammalian evolutionary morphology: A tribute to Frederick S. Szalay* (pp. 347–360). Springer.

Moore, W. J. (1980). *The Mammalian skull*. Cambridge University Press.

Murphy, W. J., Foley, N. M., Bredemeyer, K. R., Gatesy, J., & Springer, M. S. (2021). Phylogenomics and the genetic architecture of the placental mammal radiation. *Annual Review of Animal Biosciences*, *9*, 29–53.

Nomina Anatomica Veterinaria. (2017). *Nomina Anatomica Veterinaria* (6th ed.). Editorial Committee.

O'Leary, M. A., Bloch, J. I., Flynn, J. J., Gaudin, T. J., Giallombardo, A., Giannini, N. P., Goldberg, S. L., Kraatz, B. P., Luo, Z.-X., Meng, J., Ni, X., Novacek, M. J., Perini, F. A., Randall, Z., Rougier, G. W., Sargis, E. J., Silcox, M. T., Simmons, N. B., Spaulding, M., Velazco, P. M., Weksler, M.,

Wible, J. R., & Cirranello, A. L. (2013). The placental mammal ancestor and the post-KPg radiation of placentals. *Science*, *339*(6120), 662–667.

Parker, W. K. (1885). On the structure and development of the skull in the Mammalia. Part III. Insectivora. *Philosophical Transactions of the Royal Society of London*, *176*, 121–275 39 plates.

Presley, R. (1979). The primitive course of the internal carotid artery in mammals. *Acta Anatomica*, *103*, 238–244.

Rougier, G. W., & Wible, J. R. (2006). Major changes in the mammalian ear region and basicranium. In M. T. Carrano, T. J. Gaudin, R. W. Blob, & J. R. Wible (Eds.), *Amniote paleobiology: Perspectives on the evolution of mammals, birds, and reptiles* (pp. 269–311). University of Chicago Press.

Schuffeldt, R. W. (1911). The skeleton in the flying lemurs, Galeopteridae. *Philippine Journal of Science*, *6*(139–165), 185–211.

Segall, W. (1970). Morphological parallelisms of the bulla and auditory ossicles in some insectivores and marsupials. *Fieldiana Zoology*, *51*, 169–205.

Silcox, M. T., Gunnell, G. F., & Bloch, J. I. (2020). Cranial anatomy of *Microsyops annectens* (Microsyopidae, Euarchonta, Mammalia) from the middle Eocene of northwestern Wyoming. *Journal of Paleontology*, *94*, 979–1006.

Stafford, B. J. (2005). Order Dermoptera. In D. E. Wilson & D. M. Reeder (Eds.), *Mammal species of the world: A taxonomic and biogeographic reference* (3rd ed., p. 110). Johns Hopkins University Press.

Strandring, S. (Ed.). (2008). *Gray's anatomy* (40th ed.). Churchill Livingstone.

Wible, J. R. (1986). Transformations in the extracranial course of the internal carotid artery in mammalian phylogeny. *Journal of Vertebrate Paleontology*, *6*, 313–325.

Wible, J. R. (1987). The eutherian stapedial artery: Character analysis and implications for superordinal relationships. *Zoological Journal of the Linnean Society*, *91*, 107–135.

Wible, J. R. (1990). Petrosals of Late Cretaceous marsupials from North America, and a cladistic analysis of the petrosal in therian mammals. *Journal of Vertebrate Paleontology*, *10*, 183–205.

Wible, J. R. (1993). Cranial circulation and relationships of the colugo *Cynocephalus* (Dermoptera, Mammalia). *American Museum Novitates*, *3072*, 1–27.

Wible, J. R. (2003). On the cranial osteology of the short-tailed opossum *Monodelphis brevicaudata* (Didelphidae, Marsupialia). *Annals of Carnegie Museum*, *72*, 137–202.

Wible, J. R., & Hopson, J. A. (1993). Basicranial evidence for early mammal phylogeny. In F. S. Szalay, M. J. Novacek, & M. C. McKenna (Eds.), *Mammal phylogeny: Mesozoic differentiation, multituberculates, monotremes, early therians, and marsupials* (pp. 45–62). Springer Verlag.

Wible, J. R., & Martin, J. R. (1993). Ontogeny of the tympanic floor and roof in archontans. In R. D. E. MacPhee (Ed.), *Primates and their relatives in phylogenetic perspective* (pp. 111–148). Plenum Press.

Wible, J. R., Novacek, M. J., & Rougier, G. W. (2004). New data on the skull and dentition of the Mongolian Cretaceous eutherian mammal *Zalambdalestes*. *Bulletin of the American Museum of Natural History*, *281*, 1–144.

Wible, J. R., Rougier, G. W., Novacek, M. J., & Asher, R. J. (2009). The eutherian mammal *Maelestes gobiensis* from the Late Cretaceous of Mongolia and the phylogeny of Cretaceous Eutheria. *Bulletin of the American Museum of Natural History*, *327*, 1–123.

Wible, J. R. (2011). On the treeshrew skull (Mammalia, Placentalia, Scandentia). *Annals of Carnegie Museum*, *79*, 149–230.

Wible, J. R., & Shelley, S. L. (2020). Anatomy of the petrosal and middle ear of the brown rat, *Rattus norvegicus* (Berkenhout, 1769) (Rodentia, Muridae). *Annals of Carnegie Museum*, *86*, 1–35.

Wible, J. R., & Shelley, S. L. (2021). The element of Paaw in marsupials and the ear region of *Philander opossum* (Linnaeus, 1758) (Didelphimorphia, Didelphidae). *Annals of Carnegie Museum*, *87*, 1–35.

Wible, J. R., Shelley, S. L., & Rougier, G. W. (2018). The mammalian parasphenoid: Its occurrence in marsupials. *Annals of Carnegie Museum*, *85*, 113–164.

How to cite this article: Wible, J. R. (2023). The ear region of the Philippine flying lemur *Cynocephalus volans* (Placentalia, Dermoptera). *The Anatomical Record*, 1–19. https://doi.org/10.1002/ar.25174